

MULTICOMPONENT MODELS FOR THE DYNAMIC EVOLUTION OF GLOBULAR CLUSTERS

HYUNG MOK LEE

Canadian Institute for Theoretical Astrophysics, University of Toronto; and Department of Earth Sciences, Pusan University

AND

GREGORY G. FAHLMAN AND HARVEY B. RICHER

Department of Geophysics and Astronomy, University of British Columbia

Received 1989 August 28; accepted 1990 July 9

ABSTRACT

The Fokker-Planck equation has been integrated to produce a series of numerical models describing the dynamical evolution of globular clusters with a mass spectrum. Three-body binary heating is included to obtain postcollapse evolution and a steady Galactic tidal field is imposed. Since no direct interactions between stars (such as tidal captures or mergers) are considered, the models are appropriate for globular clusters with a relatively low mass ($M \leq 10^5 M_{\odot}$). A wide range of initial mass functions is considered and the evolution of the mass function is examined. The mass function begins to change appreciably during the postcollapse expansion phase due to the selective evaporation of low-mass stars through the tidal boundary. One signature of highly evolved clusters is thus a significant flattening of the mass function. The age measured by the half-mass relaxation time increases very rapidly from a characteristic value of ~ 100 at the final stage of disruption. This appears to be consistent with the sharp cutoff near 10^8 yr in the distribution of the half-mass relaxation times for the Galactic globular clusters. We also consider the evolution of clusters containing massive dark remnants (i.e., white dwarfs or neutron stars). The efficient formation of three-body binaries among the degenerates and the relative flattening of the luminosity profile compared to the density profile, lead to postcollapse models with a sufficiently low concentration that the core may be resolvable.

Subject headings: clusters: globular — luminosity function — stars: stellar dynamics

I. INTRODUCTION

Theoretical studies of the dynamical evolution of stellar systems have concentrated mainly on single or few mass component models because of their simplicity. For many globular clusters, CCD photometry is now available to well below the main-sequence turnoff point and the corresponding partial mass functions have been derived (see McClure *et al.* 1986). Recently, Fahlman *et al.* (1989) have reported observations of the mass function in NGC 6397 which extend essentially to the hydrogen burning limit. More realistic models are clearly needed in order to compare the theoretical results with the observed properties of such well-studied globular clusters.

The interpretation of an observed mass function is not straightforward because it need not reflect the initial mass function (IMF) but rather, some complicated result of dynamical evolution. In addition, one usually derives the mass function from data obtained at a limited range of radial distances from the cluster center. If the relaxation time scale is sufficiently short, the local mass function will generally be different from the global mass function because of mass segregation. Multi-mass King models may be used to infer the global mass function from local observations (see Pryor, Smith, and McClure 1986) but the applicability of such models to real clusters has not been studied carefully.

There are many physical processes which should be incorporated in realistic models for the evolution of globular clusters. These include the initial mass function, stellar evolution, dynamical relaxation, physical interactions between single and binary stars, and external effects, such as the Galactic tidal field and the occasional tidal shock. It is a very complicated matter to put all these effects into a single model. In a remarkable study, Stodolkiewicz (1985) developed a model, based on Monte Carlo simulations, in which almost all conceivable

effects are included. Unfortunately, statistical fluctuations and the complex nature of the solution are obstacles in obtaining a clear picture of cluster evolution from this work. One also has to recognize the difficulty in choosing initial conditions when the model requires a very detailed specification of many parameters.

There have been efforts to investigate separately the effects listed above. The role of physical encounters between stars, including binaries formed by either tidal capture or three-body processes, has been studied by Ostriker (1985), McMillan (1986), Statler, Ostriker, and Cohn (1987), and Lee (1987*a*, *b*) among others. The steady Galactic field is modeled by Lee and Ostriker (1987) and Chernoff and Shapiro (1988). The evolution of multicomponent clusters, including the dynamical effects of stellar evolution, has been studied by Chernoff and Weinberg (1990).

The purpose of the work reported here is to study the long-term evolution of globular clusters and to examine some of the observational implications. To this end, we have combined a few of the above effects, as described below, in a series of models which remain simple enough that a clear picture can be drawn from the numerical results.

Since any given cluster reaches core collapse in a finite time, the outer parts of the cluster, where the relaxation time scale is very long, are essentially frozen and, at the time of collapse, will simply reflect their initial condition. Postcollapse models are necessary in order to follow the long-term evolution. Three-body binary heating, which is simpler to treat than tidally captured binaries, is used in our models to obtain the postcollapse expansion. These models are thus applicable mainly to relatively low mass clusters, $M \leq 10^5 M_{\odot}$, since the neglected physical interactions between stars (e.g., the formation of tidally captured binaries and stellar mergers) become impor-

tant in higher mass clusters. During the expansion, stars in the outer part of the cluster pass through the tidal boundary defined by the location of the cluster in the Galaxy. These losses will change the mass function because low-mass stars are preferentially removed. We impose a tidal boundary condition in our models in order to investigate the evolution of the mass function. To summarize: our models include an initial mass function, three-body binary heating, and a steady Galactic tidal field. We employ the orbit-averaged Fokker-Planck technique, which requires modest computing time and yet is suitable for studying the dynamical evolution of large stellar systems. The code used here is based upon that described in Statler, Ostriker, and Cohn (1987).

In the next section, the assumptions and initial conditions of the models are described in more detail. The numerical results and theoretical interpretations are given in § III. We discuss the implications of our results for observations in § IV. The final section summarizes our major findings.

II. INITIAL CONDITIONS AND ASSUMPTIONS

a) Mass Function

In order to make our computations simpler, we do not include the evolution of primordial high-mass stars. Stellar evolution has the effect of slowing down the dynamical evolution, and it may even destroy the whole cluster on a relatively short time scale if there are a sufficiently large number of high-mass stars in the IMF (Chernoff and Weinberg 1990). The steep dependence of the main-sequence evolution time scale on stellar mass ensures that most of the stellar evolution takes place within a much shorter time than any interesting dynamical time scale. Thus, to a first approximation, we may assume that stellar evolution has the effect of changing only the initial condition in which the cluster begins its dynamical evolution. For example, a cluster with an initial mass spectrum described by a power-law index of $x = 1$ (see eq. [1] below) and extending between $0.1 M_{\odot}$ and $15 M_{\odot}$ will lose almost 30% of its initial mass within 2×10^8 yr as the stars down to $3 M_{\odot}$ evolve. Implicitly, our simulations begin at about this point. The evolution of the stars from $3 M_{\odot}$ to $1 M_{\odot}$ will lead to a mass loss of only $\sim 12\%$ extending over 6×10^9 yr, which is many half-mass relaxation time scales for our models, and is ignored. The dynamical effect and the change in the mass function due to the evolution of the remaining low-mass stars is assumed to be negligibly small.

The initial mass function for the main-sequence stars is assumed to be a power law. Massive degenerate remnants, representing neutron stars or white dwarfs, have been added in some models. We will call these stars "primordial" degenerates to indicate that they are formed in the very early phase of dynamical evolution. The number of neutron stars can be estimated by extrapolating the present mass function but the actual number remaining in the cluster may be only a small fraction of such evolved stars. The translational energy obtained during the final stage of stellar evolution as a result of small deviations from spherical symmetry is sufficient to eject the star from the shallow gravitational potential of the globular clusters.

Similarly, the number of white dwarfs may be estimated by extrapolating the main-sequence mass function and using, for example, the initial-final mass relation of Iben and Renzini (1983). Only those remnants more massive than the present-day main-sequence turnoff stars are of interest in this dynamical

study. However, there is some question as to whether an extrapolation of the observed mass functions, particularly those which are relatively flat, is reasonable (see e.g., Meylan 1988; Pryor *et al.* 1989).

Because of such uncertainties, we assume here that the number of massive degenerate stars in the initial models is simply a free parameter to be chosen in addition to the form of the main-sequence mass function. For simplicity, the degenerate stars are assigned the same individual mass. Thus the number of stars between m and $m + dm$ is

$$\begin{aligned} N(m)dm &= C_1 m^{-(1+x)} dm, \quad m_{\min} < m < m_{\max}, \\ &= C_2 \delta(m - m_{\text{deg}}) dm, \quad m > m_{\max}, \end{aligned} \quad (1)$$

where m_{\min} and m_{\max} are the minimum and maximum (i.e., turnoff) mass of the main-sequence stars and m_{deg} is the mass of the degenerate stars and δ is the Kronecker δ -function. Note that $m_{\text{deg}} > m_{\max}$ in those models containing degenerate stars.

The number of mass groups used in the present study is seven. The dynamic range is $m_{\min}/m_{\max} = 7$ with linear spacing for models consisting of main-sequence stars only. In models containing a primordial degenerate component, we keep the same dynamic range for the main-sequence stars but distribute them in six mass bins and use the remaining mass class for the degenerates. More mass species should be used if accurate results for core-collapse time scales are desired (Chernoff and Weinberg 1990) but note that the time to reach core collapse is only a small fraction of the overall evolution time scale considered here. The postcollapse evolution is much less sensitive to the number of mass classes because near equipartition is maintained among the different mass stars. Hence, the equipartition process, which is a critical factor in the initial core collapse, is not significant in the postcollapse evolution. Computations made with 10 or more mass classes were found to produce essentially the same results as the seven component models used in this study. The smaller number of mass classes adopted here in the interests of economy should be adequate to investigate the long term evolution of multi mass clusters.

The initial density distribution is assumed to be that of a single-component King model. We have used two values for the central potential of these models: $W_0 = 4$, representing a relatively open initial density distribution and $W_0 = 7$, representing a more concentrated initial density distribution.

b) The Tidal Field

We have assumed that the Galactic tidal force acting on a cluster is constant. This is clearly unrealistic since the majority of the globular clusters are expected to have noncircular orbits. Furthermore, the clusters should experience occasional tidal shocks as they pass through the Galactic disk or other dense regions. Nevertheless, a steady Galactic tidal field is adopted for simplicity and may be regarded as the average tidal field felt by the cluster as it moves along its noncircular orbit. The numerical N -body study by Allen and Richstone (1988) indicates that the tidal boundary of globular clusters is mainly determined by the perigalactic passage.

The treatment of the tidal boundary condition is the same as in Lee and Ostriker (1987). The distribution function beyond the tidal energy is decreased according to the following equation:

$$\frac{df(E)}{dt} = -C_3 f(E) \{ [1 - (E/E_t)^3]^{1/2} / t_{\text{tid}} \}, \quad E < E_t, \quad (2)$$

where E_t is the tidal energy (equivalent to the gravitational potential at the tidal boundary). C_3 is an adjustable parameter, nominally of order unity, which is discussed further below. The gravitational potential is defined as a positive quantity and is zero at infinity. The tidal time scale t_{tid} for a cluster of mass M and tidal radius R_t is defined by

$$t_{\text{tid}} \equiv \frac{2\pi}{\sqrt{(4\pi/3)G\rho_t}}, \quad (3)$$

where ρ_t is the mean density within the tidal radius. This is a fixed quantity throughout the evolution under our assumption of a steady Galactic tidal field. Also note that t_{tid} is equivalent to the orbital time scale for a cluster moving in a circular orbit at the Galactocentric distance where the tidal field is determined.

c) Binary Heating

For relatively massive stellar systems, Ostriker (1985) demonstrated that the physical interactions involving tidally captured binaries are dynamically more important than the binaries formed through three-body processes. However, the situation in multicomponent models is likely to be different because of mass segregation and equipartition among different mass stars. The presence of massive degenerate stars makes the three-body binaries more important because compact stars would feel no tidal effects (see, for example, Lee 1987a).

The method of incorporating the dynamical effects of three-body binaries in the Fokker-Planck scheme has been described by Lee (1987a, b) and Cohn, Hut, and Wise (1989). Lee (1987a) found that the explicit inclusion of the formation, hardening, and ejection of three-body binaries would provide identical results to those obtained by the more indirect method described by Lee (1987b) and, more recently, by Cohn, Hut, and Wise (1989). In the indirect method, an individual binary is assumed to release a certain amount of energy to the cluster through both hardening and ejection, but these processes are not directly followed. Note that the time-averaged number of binaries in single component models is 5 or fewer and that this number does not change during the postcollapse phase (Lee 1987a). We anticipate that the number of binaries in our multicomponent models is also of order unity. Hence, a real cluster heated by three-body binaries will be subject to statistical fluctuations which are not reflected in the smooth solutions to the Fokker-Planck equation.

The treatment of three-body binaries is still very complicated in multicomponent models because there are a large number of combinations to be considered in the formation of the binaries and for the interactions between the binaries and the other stars. Therefore, we adopt the following simplifications (based on suggestions made jointly by P. Hut and D. C. Heggie). The total heating rate per unit volume by three-body binaries is assumed to have the form

$$\dot{E}_{\text{tot}} = C_4 G^5 \left(\sum_i \frac{n_i m_i^2}{v_i^3} \right)^3 v_c^2, \quad (4)$$

where n_i , m_i , and v_i are number density, mass, and velocity dispersion, respectively, of each component, and v_c is the mass weighted central velocity dispersion. The constant C_4 is taken to be 4.21×10^3 from Cohn (1985).¹ Equation (4) is the product of the binary formation rate per unit volume and the average amount of energy released per binary before it is ejected. The energy released is assumed to be proportional to

the central velocity dispersion. The binary formation rate is computed by taking the probability for any three stars to be within $p \approx Gm/v^2$ during the time interval $\Delta t \approx (np^2v)^{-1}$ (Binney and Tremaine 1988, chap. 8). The heating is then distributed to each mass component proportional to the density such that

$$\dot{E}_i = \frac{\rho_i}{\rho_{\text{tot}}} \dot{E}_{\text{tot}}, \quad (5)$$

where ρ_{tot} is the total density. Such an effect can be included in the Fokker-Planck equation by computing a heating coefficient

$$H(E) = \frac{\int_0^{\Phi^{-1}(E)} dr v r^2 \dot{E}_{\text{tot}} / \rho_{\text{tot}}}{\int_0^{\Phi^{-1}(E)} v r^2 dr}, \quad (6)$$

and adding this to the first-order Fokker-Planck coefficient, as described by Lee (1987b), and Cohn, Hut, and Wise (1989). By making the mass function almost a δ -function, we have verified that our code gives results in agreement with those reported by Cohn, Hut, and Wise (1989). The results are also in accord with those of Heggie and Ramamani (1989) who performed similar calculations with a gaseous model.

In the following section, we discuss the models with a strict power-law mass function for the purpose of understanding the general behavior of multimass models. The models with degenerate stars are perhaps more appropriate for comparison with the observed globular clusters where some dark remnants are believed to be present. These are discussed in § IVc.

III. NUMERICAL RESULTS

a) Model Parameters

In order to calculate models, we have to specify the total mass of the cluster, M_0 ; the minimum and the maximum mass, m_{min} and m_{max} ; the adjustable constants C_1 , C_2 , and C_3 ; the mass spectral index, x ; and the central potential, W_0 , of the initial King model. For the models with main-sequence stars only, $C_2 = 0$. The tidal evaporation constant is set to $C_3 = 1$ for all the models presented here, but the results are insensitive to the choice of C_3 as long as it is of order of unity. We have taken $m_{\text{max}} = 0.7 M_\odot$ which is close to the turnoff mass in a globular cluster and $m_{\text{min}} = 0.1 M_\odot$, which is just above the hydrogen burning limit for population II stars. The total mass of the models is $M_0 = 1.3 \times 10^4 M_\odot$ unless otherwise specified. Three different values for the mass spectral index are used; $x = 1, 2$, and 3 . The constant C_1 is determined when M_0 and x are specified.

b) Gravothermal Oscillations

It is well known that some postcollapse models are susceptible to nonlinear gravothermal oscillations which affect the central regions of the models. These oscillations are artificially suppressed by adopting integration time steps which are much longer than the central relaxation time scale. In this case, monotonically evolving solutions are obtained.

Goodman (1986) found that a postcollapse cluster containing only a single mass species and powered by three-body binaries is unstable against gravothermal oscillations if

¹ The difference between Cohn's value $C_4 = 90$ and the value given here is due to the fact that Cohn used the one-dimensional velocity dispersion whereas we have used the three-dimensional one here.

$N > 7000$, where N is the number of stars. This result has been confirmed by Heggie and Ramamani (1989) using a gas-dynamical approach and by Cohn, Hut, and Wise (1989) using a Fokker-Planck code.

The appearance of gravothermal oscillations in multimass models has not been extensively investigated. Murphy, Cohn, and Hut (1989) reported that such oscillations are strongly suppressed in their multimass models. For example, their model with $m_{\min} = 0.1 M_{\odot}$, $m_{\max} = 1.2 M_{\odot}$ did not show oscillations until the number of stars exceeded 5×10^5 . It is not too difficult to understand these results: the core of the multimass models is dominated by a small number of high-mass stars which essentially constitute a small N -body system.

In a recent preprint, Murphy, Cohn, and Hut (1990) have shown that multimass models do show gravothermal oscillations when the total cluster mass exceeds some threshold which varies with the mass spectral index. We did not observe gravothermal oscillations in a few selected models with $M_0 = 1.3 \times 10^4 M_{\odot}$, which is consistent with their findings. Note that most of the results discussed in this paper are based on these relatively low mass models. However, we also discuss some models with substantially larger masses ($\geq 10^5 M_{\odot}$) and these, when integrated with a sufficiently small time step, are unstable to gravothermal oscillations, again in accord with the results of Murphy, Cohn, and Hut (1990). Unfortunately, it is not practical to use such small time steps to investigate the long term evolution of interest in this paper. All the results reported here are based on integrations with a time step which suppresses the appearance of gravothermal oscillations.

We have performed a small number of experiments to compare the evolution of the same model calculated with and without resolution of the gravothermal oscillations (i.e., with long and short time steps). The results, which necessarily apply only over limited time intervals, indicate that the long time step integrations do track the changes in the more global cluster parameters; e.g., the total mass and the half-mass radius. This is not too surprising because the oscillations are closely confined to the cluster center and strongly affect only a tiny fraction, very much less than 1%, of the total cluster mass (see e.g., Murphy, Cohn, and Hut 1990). Hence we do not expect that the long-term evolution of models which exhibit gravothermal oscillations when integrated with short time steps would differ substantially from the result obtained using longer time steps which suppress the appearance of the oscillations. This issue, however, certainly warrants further study.

c) Disruption

There are several mechanisms by which stars might escape from the stellar system: (1) ejection through binary-single or binary-binary interactions, (2) evaporation of high-velocity stars through dynamical relaxation, and (3) diffusion of stars across the tidal boundary due to the general expansion of the cluster. The number of ejections is expected to be very small because the number of binaries formed during the cluster evolution is very small. The dynamical evaporation cannot be treated in the orbit-averaged Fokker-Planck scheme, but it is a small fraction of the diffusion loss (see Lee and Ostriker 1987 for a detailed discussion).

Figure 1 displays the change of mass in time for the $W_0 = 7$ models with different initial mass functions: $x = 0$, $x = 1$, and $x = 2$. The total mass is fixed at $M_0 = 1.3 \times 10^4 M_{\odot}$. The corresponding models with $W_0 = 4$ or with a different M_0 would show no visible difference in the evolution of total mass.

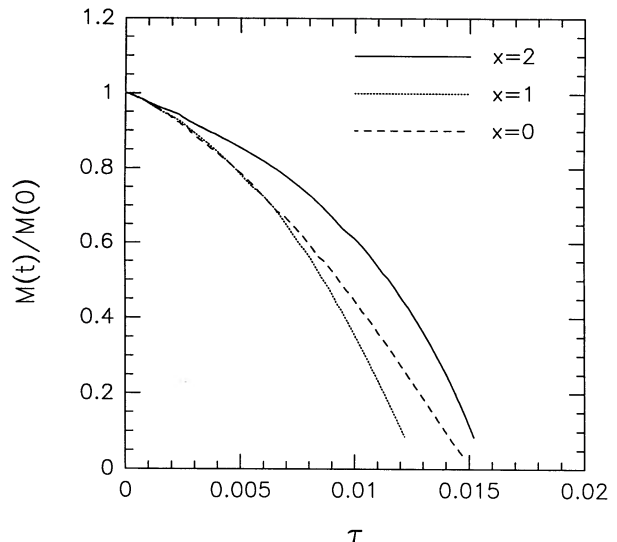


FIG. 1.—The evolution of the total mass for three models with different initial mass functions: $x = 0$, $x = 1$, and $x = 2$. In all three cases, the central potential of the initial King model was $W_0 = 7$, and the initial mass was $M_0 = 1.3 \times 10^4 M_{\odot}$. The results, however, are insensitive to either the initial density distribution or the initial mass.

The dimensionless time scale used in this and other figures is

$$\tau \equiv \left(\frac{t}{t_{\text{tid}}} \right) \left(\frac{\ln \Lambda}{N} \right), \quad (7)$$

where N is the *initial* number of stars in the cluster and $\Lambda = 0.4N$.

We followed the evolution of the cluster until the numerical instability makes further integration impossible. At the final step, the mass of the cluster is typically $\sim 5\%$ of the initial mass. The time of complete disruption τ_{ev} obtained from extrapolation of the Figure 1 is found to lie between 0.013 and 0.016. We found that τ_{ev} mainly depends on the form of the initial mass function and is very insensitive to the initial total mass or W_0 for the clusters with the same form of the initial mass function. We also found that the choice of C_3 in equation (2) does not affect the evolution as long as it is of order of unity. This is because the orbital time scale for the stars near the tidal boundary (i.e., t_{tid} in eq. [3]) is much shorter than the evolution time scale for the cluster (i.e., relaxation time scale).

The mass decreases nearly linearly with time for postcollapse clusters experiencing self-similar evolution (Henon 1961). Although the structure of our models changes continuously during the expansion, the outer part becomes more or less self-similar at late times (i.e., the ratio between the half-mass radius and the tidal radius becomes constant). Under this condition, the mass evaporation rate becomes a constant, leading to nearly linear decrease in mass which is seen in Figure 1.

d) Central Density and Velocity Dispersion

The evolution of the central density is shown in Figure 2, for models with different IMFs ($x = 1$ and $x = 2$) and different initial concentrations ($W_0 = 4$ and 7). The initial mass of the clusters is fixed at $M_0 = 1.3 \times 10^4 M_{\odot}$ in all cases shown in this figure. The unit of density is $M_0/r_c^3(0)$, where M_0 and $r_c(0)$ represent the initial mass and core radius of the model. Due to the presence of the tidal boundary, the density does not show the power-law behavior characteristic of quasi-statically evol-

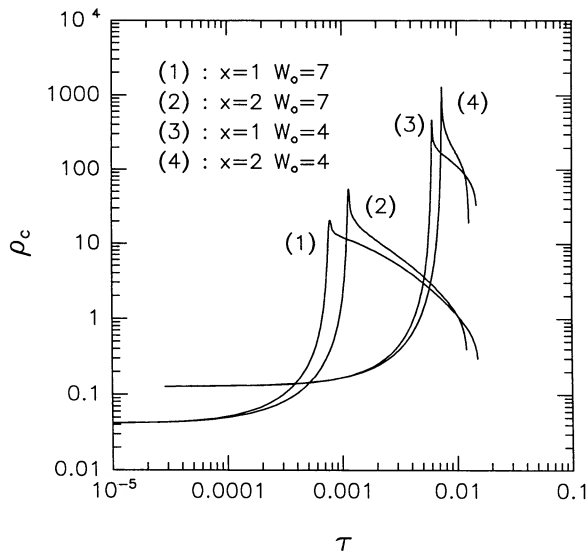


FIG. 2.—The evolution of central density ρ_c for four models as indicated on the figure. The initial mass was $1.3 \times 10^4 M_\odot$ in all cases.

ing isolated clusters. Following the arguments of Goodman (1988), and Lee, Heggie, and Ostriker (1990), we can relate the evolution of the central density with other physical parameters based on the requirement that the energy generated in the core must be equal to the global rate of energy change. We will assume that the central density is dominated by the highest mass component, which also receives most of the three-body binary heating.

The energy generation rate in the core is (e.g., Goodman 1988)

$$\dot{E}_{\text{core}} \propto \rho_c^2 v_c^{-7} M_c \propto \rho_c^3 v_c^{-7} r_c^3, \quad (8)$$

where M_c ($\approx \frac{2}{3}\pi\rho_c r_c^3$) is the core mass and r_c is the core radius defined by

$$r_c \equiv \sqrt{\frac{3v_c^2}{4\pi G\rho_c}}. \quad (9)$$

The rate of change in the total energy, on the other hand, is

$$\dot{E} \approx -\frac{d}{dt} \left(\frac{0.2GM^2}{r_h} \right) \propto \frac{GM^2}{r_h} \frac{1}{t_{\text{rh}}}. \quad (10)$$

The half-mass relaxation time scale is defined by (Spitzer and Hart 1971)

$$t_{\text{rh}} \equiv \frac{M^{1/2} r_h^{3/2}}{6.7G^{1/2} \langle m \rangle \ln \Lambda}, \quad (11)$$

where $\langle m \rangle$ is the mean mass per star. By setting equation (8) equal to equation (10), we obtain the following algebraic relation for the central density

$$\rho_c \propto \frac{M^{3/2}}{r_h^{5/3}} \langle m \rangle v_c^{-8/3} \propto M^{7/3} r_h^{-3} \langle m \rangle^{2/3}, \quad (12)$$

where we have used the relationship $v_c^2 \propto GM/r_h$.

In Figure 3, we have plotted the evolution of ρ_c for the model with $x = 2$ and $W_0 = 7$. Values of ρ_c calculated at selected times from the right-hand side of equation (12) are shown as filled circles. The unknown constant implicit in equation (12)

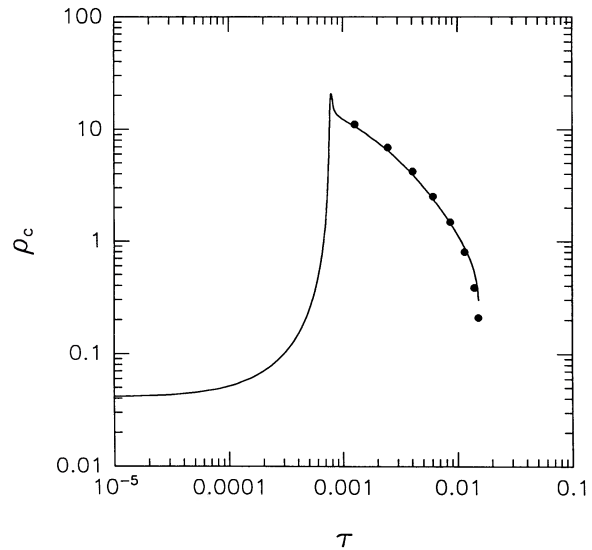


FIG. 3.—The evolution of the central density in model 2 of Fig. 2 (curve), compared to the results (filled circles) obtained by applying the scaling relationship given in eq. (12) of the text.

has been fixed to match the numerical results. Note that we had to use the time-dependent behavior of r_h , $\langle m \rangle$, (calculated for all stars within r_c), and the total mass M obtained from the numerical integrations in order to get the relation shown in Figure 3. The consistency of equation (12) with the numerical results supports the idea that the physical parameters are determined by the assumed energy balance, but that principle is not sufficient to derive the behavior of postcollapse clusters without going through the numerical integration.

The behavior of the mass-weighted central velocity dispersion, in units of $GM_0/r_c(0)$, is shown in Figure 4 for the model (1) shown in Figure 2. The precollapse evolution is characterized by the tendency toward equipartition among the various

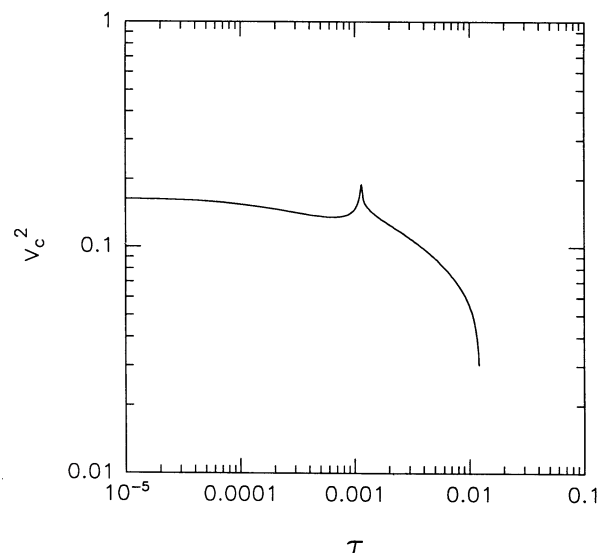


FIG. 4.—The evolution of the central velocity dispersion (weighted by stellar mass) for model 1 of Fig. 2. The decrease of v_c during the precollapse evolution is due to mass segregation and energy equipartition.

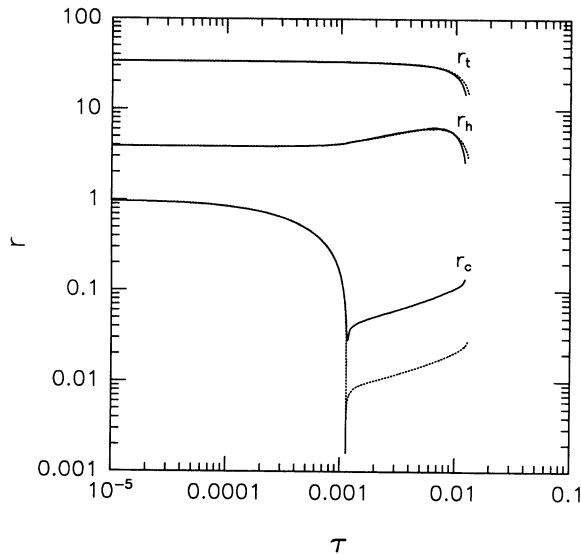


FIG. 5.—The evolution of the tidal, half-mass and core radii for the same model shown in Fig. 4. Also plotted as a dotted line is the evolution of core radius for a model with 10 times higher initial mass (i.e., $M_0 = 1.3 \times 10^5 M_\odot$), but otherwise identical. Note that the tidal and half-mass radii are the same regardless of the initial mass.

mass components. Therefore the mass-weighted velocity dispersion is *decreasing* with time during the core collapse in contrast to the slow increase observed in single component models.

The core radius, the half-mass radius, and the tidal radius, expressed in units of the initial core radius, are shown in Figure 5 for the same model appearing in Figure 4. The dotted lines show these radii for a model in which the initial mass was increased by a factor of 10, to $M_0 = 1.3 \times 10^5 M_\odot$, but which is otherwise identical. Note that the half-mass and the tidal radii are not affected by the change of initial mass but that the core radius is sensitive to this parameter. The scaling of the core radius with the total number of stars also follows Goodman's (1987) similarity solution for single mass component, isolated clusters heated by three-body binaries; i.e., $r_c \propto N^{-2/3}$.

The higher mass model is unstable to gravothermal oscillations which have been suppressed in the calculations reported here. The numerical experiments described earlier indicate that the central density obtained from the long time-step integrations is some time-weighted average value when compared to the corresponding oscillating solution. As expected, our computed central density is close to the value appropriate to the phases of maximum expansion, the state in which the oscillating model spends most of its time. Hence our results describe what might be termed a "most probable" view of the cluster. Further discussion of the appearance of a cluster experiencing gravothermal oscillations may be found in Murphy, Cohn, and Hut (1990).

Since the the core-radius increases in time while the tidal radius decreases (very slowly), the concentration parameter $c [\equiv \log(r_t/r_c)]$ decreases with time. However, in the case where $M_0 = 1.3 \times 10^5 M_\odot$, the concentration parameter remains very high until complete disruption of the cluster. The high degree of concentration has been understood to be a characteristic of models for postcollapse clusters. On the other hand, the *observed* core radius is located at the point where the

surface brightness has fallen by a factor of $1.5 \sim 2$ from its central value. (To avoid confusion with terminology, we will call this point the half-brightness radius, denoted by r_{hb}). If there are massive degenerate stars with negligible luminosity, the half-brightness radius could be quite different from the core radius (which is very close to the radius where the surface mass density is half of its central value). This point, first mentioned in the context of postcollapse evolution by Inagaki and Lynden-Bell (1983) and explored in some detail by Larson (1984), is discussed further in the following section.

IV. OBSERVATIONAL IMPLICATIONS

a) Distribution of Half-Mass Relaxation Times

There is fairly good evidence that the ages of most of the globular clusters are close to the Hubble time and that their spread in age is sufficiently small that we may assume they are coeval. During core collapse, the half-mass relaxation time hardly changes. Since core collapse takes place within ~ 10 initial half-mass relaxation time units, the age of a cluster must be less than this order for it to be in a precollapse phase. The half-mass relaxation time for most Galactic globular clusters lies between $10^{7.5}$ and 10^{11} yr (Spitzer 1988, p. 6; Binney and Tremaine 1988, p. 515). We expect those clusters with short half-mass relaxation time scales to be in a postcollapse phase (unless stellar evolution has prolonged the core-collapse phase significantly; see e.g., Chernoff and Weinberg 1990).

We have plotted the ages of the model clusters, measured in units of their half-mass relaxation time, versus time in Figure 6. The models shown here are those of Figure 1, and they all reach core collapse in a few initial half-mass relaxation times. Note that the evolution shown in this figure depends only on the adopted IMF; models with different M_0 or different W_0 but the same IMF would follow nearly identical tracks in this figure. During the postcollapse expansion, t/t_{rh} increases slowly, reaching $t/t_{rh} \simeq 100$, and then increases very rapidly as complete disruption is approached. Also notice that the behav-

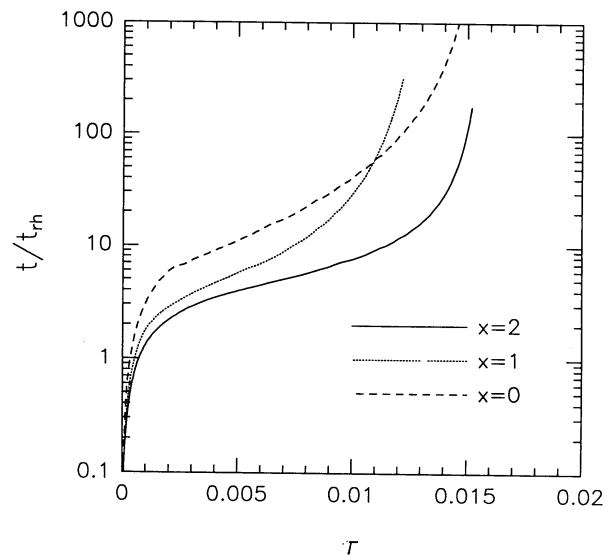


FIG. 6.—The evolution of the age in units of the present half-mass relaxation time for the same three models appearing in Fig. 1. In all cases t/t_{rh} increases rapidly beyond ~ 100 , although the case with flatter mass function tends to show a gentler change. The behavior of t/t_{rh} depends mainly on the initial mass function and is very insensitive to either M_0 or W_0 .

ior of t/t_{rh} is gentler for the shallower IMF than it is for the steeper ones. For $x = 0$, t/t_{rh} varies rather slowly, even after reaching ~ 100 .

Considering these results, we suggest that those clusters whose present half-mass relaxation time scale is small (i.e., t/t_{rh} is large) may be in the disruption phase. We expect to see only a small number of such clusters because of the rapid change in t/t_{rh} just before complete disruption occurs. This is consistent with the near absence of Galactic globular clusters with t_{rh} less than $\sim 10^8$ yr.

It would be interesting to see if there is other support for this speculation. As the end of dynamical evolution is approached, most stars remaining in the cluster are relatively massive and, therefore, we anticipate a dramatic change in the mass function. This subject is discussed below.

b) Evolution of the Mass Function

Mass segregation has the effect of concentrating the high-mass stars in the cluster core while the low-mass stars are pushed to the outside. As a result, the stars leaving the tidal boundary are mostly low-mass stars and thus, they are progressively depleted from the IMF. For numerical convenience, we define a normalized mass function, $\tilde{N}(m)$ such that $\sum_i \tilde{N}(m) = 1$, with the mass unit chosen to be m_{min} , the mass of the lowest mass component included in the models. We have shown the global mass functions, $\tilde{N}(m)$, at different epochs in Figure 7a, and the mass function measured within the half-mass radius, $\tilde{N}_h(m)$, in Figure 7b, for the model with $x = 1$ and $W_0 = 4$. Again, neither the initial density distribution nor the initial mass affects the general behavior of the mass function at later times.

The mass function within the half-mass radius changes faster than the global one. While $\tilde{N}(m)$ remains almost frozen during the collapse, $\tilde{N}_h(m)$ experiences significant evolution even before the collapse. For this reason, we show the precollapse epoch in Figure 7b in addition to the postcollapse times appearing in Figure 7a. The flattening of the mass function is clearly visible in both cases. Even the slope of the mass func-

tion reverses for $\tilde{N}(m)$ and $N_h(m)$ at later times. Although the flattening of the mass function is a universal phenomenon, the case with the $x = 2$ IMF did not show the slope reversal except for a brief period at the end of its evolution.

Richer and Fahlman (1989) derived the mass function for M71 from CCD photometry and found that the mass function is reversed in the range between $m = 0.4$ and $0.8 M_{\odot}$. Given the fact that this cluster now has a relatively small half-mass relaxation time ($\approx 2 \times 10^8$ yr), and low total mass ($\approx 3 \times 10^4 M_{\odot}$), the present mass function may reflect tidal evaporation rather than the initial mass function.

On the other hand, the surface brightness profile of M71 is relatively open ($c \approx 1.1$) in sharp contrast to the highly concentrated postcollapse models. The concentration decreases continuously during the expansion phase (see Fig. 5) but always remains high. Note that at the end of the evolution for the model with an initial mass of $M_0 = 6 \times 10^4 M_{\odot}$ (appropriate for M71), the concentration parameter is ~ 2.2 far larger than what is observed in M71. Of course, what is observed is essentially the half-brightness radius. The model cluster may have a significantly different *appearance* if the cluster contains massive degenerate stars as discussed below.

c) Effects of Massive Degenerate Remnants

One of the criteria in identifying a collapsed cluster has been the size of the core radius (e.g., Djorgovski and King 1986). Once core collapse has been reached, the postcollapse expansion is sufficiently slow that the core radius remains unresolvable as demonstrated in Figure 5.

It is also true that the size of the core radius depends on the strength of the heating source or on the initial density distribution of the cluster: the stronger the energy source, the larger the core radius and those clusters with a small number of stars can be regarded as having a higher heating rate in a relative sense (see Goodman 1987).

The half-brightness radius (based on the surface brightness profile) can be larger than the core radius if the degenerate stars have a higher individual mass than the most massive

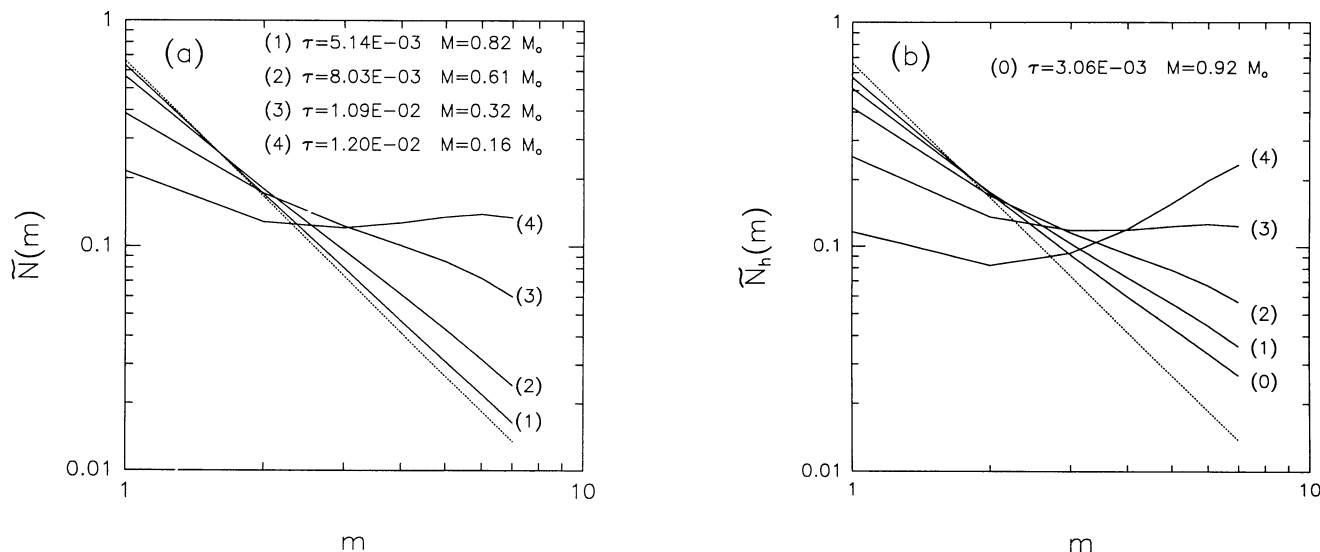


FIG. 7.—The normalized mass functions within (a) the tidal radius, $\tilde{N}(m)$ and (b) the half-mass radius, $\tilde{N}_h(m)$, at different epochs for model 3 of Fig. 2. The mass unit along the abscissa is m_{min} , the smallest stellar mass included in the model. The initial mass function is indicated by the dotted line. All epochs, τ , except that labeled (0) in (b), are postcollapse. The mass of the cluster, in units of the initial mass M_0 , is also shown for each epoch.

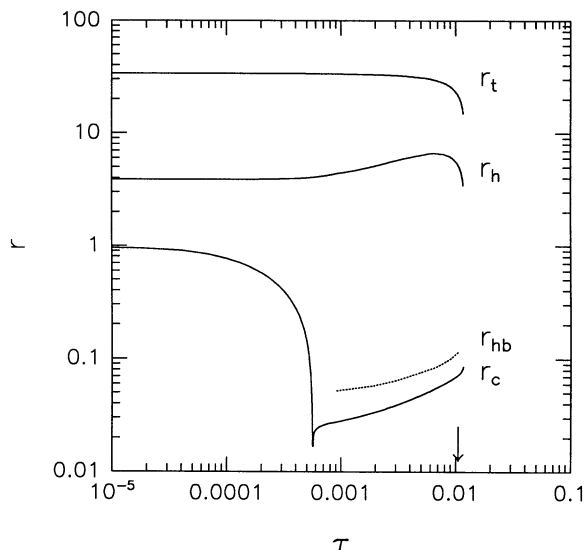


FIG. 8.—The evolution of tidal, half-mass and core radii for the model containing massive degenerates (initially 3% of the total mass). The degenerate mass is assumed to be $1.4 M_{\odot}$ while the most massive luminous stars, those at the main-sequence turnoff, have $m = 0.8 M_{\odot}$. Also indicated, by the broken line, is the half-brightness radius, r_{hb} , assuming that the observed luminosity is entirely dominated by the most massive stars. The arrow indicates the epoch of Fig. 9.

luminous star. The presence of dark remnants also boosts the heating rate significantly because the velocity dispersion of the massive stars becomes smaller than the virial value through the equipartition process (see eq. [4]). To investigate these effects, we computed the evolution of a model with an initial mass of $6 \times 10^4 M_{\odot}$, $x = 1$, $m_{deg} = 1.4 M_{\odot}$, $m_{min} = 0.114 M_{\odot}$ and $m_{max} = 0.8 M_{\odot}$. The main-sequence stars were placed in six linearly spaced mass bins. The degenerate stars comprised 3% of the initial mass of the cluster.

The evolution of the tidal, half-mass, and core radii is displayed in Figure 8. The broken line shows the half-brightness radius of the stars with m_{max} at several epochs. Essentially, it is these stars that determine the cluster luminosity profile. Evidently, the half-brightness radius is generally larger than the core radius by more than a factor of 1.5. The observed concentration parameter, based now on the half-brightness radius, becomes correspondingly smaller. In this case, it is still quite large compared with that of M71: at the final point of the calculation, $c \approx 2$. Given the many theoretical and observational uncertainties, we regard this concentration to be rather low that many low-mass clusters, may in fact be in a post-collapse phase without showing a strong cusp.² Clearly, any additional energy sources in the core during the expansion (such as stellar evolution and heating by tidally captured binaries) would help in making the core radius even larger. A significant population of more massive remnants; i.e., black holes, could also help (see Larson 1984).

We show the surface density profiles of the degenerate stars

² Recently, Fahlman, Richer, and Drukier (1990) have re-examined the star count data in the central regions of M71 and found some evidence for a very shallow power-law deviation from a King profile. However, efforts to reproduce this result with the models discussed here have not been successful. It appears that one must fine tune some of the parameters; e.g., the shape of the IMF or the fraction of heavy remnants, in order to fit a specific model to data describing this particular cluster. A more detailed discussion of this work will appear elsewhere.

(which dominate the mass at small radius) and of the highest mass luminous stars (which determine the observed surface brightness profile) in Figure 9. Both curves are normalized by the central values. The luminosity profile is significantly flattened compared to the density profile of the degenerate stars due to the relatively high mass ratio between turnoff and degenerate stars in the present model. Such flattening is very well observed in M15, and provides clear evidence for the presence of massive degenerate stars in that cluster. At the epoch shown in this figure, the degenerate stars comprise $\sim 25\%$ of the remaining mass (essentially no degenerates have escaped). The existence of such a population of dark remnants in M71 has not been ruled out by Richer and Fahlman (1989).

We conclude that even a small initial number of massive degenerates can provide a way of producing a relatively open surface brightness distribution for clusters of moderate initial mass. Deep photometric observations of other clusters with relatively low half-mass relaxation time scales would be of considerable interest.

V. SUMMARY

We have developed a series of models suitable for studying the dynamical evolution of relatively low mass globular cluster systems. Our models include an initial mass function, three-body binary heating and the Galactic tidal field. Mass segregation and the presence of the Galactic tidal field induce evolution of the mass function. Within the half-mass radius, the mass function experiences significant evolution even during the collapse phase. The lifetime of a cluster depends primarily on the tidal field and its initial mass.

The age of a cluster measured in units of the half-mass relaxation time is a monotonically increasing function of time, but the rate of increase is slow until the age reaches a value of ~ 100 . The rapid increase beyond that value may be the reason for the near absence of Galactic globular clusters with half-mass relaxation times smaller than a few times 10^7 yr: those with shorter relaxation times would be disrupted very quickly. This also implies that the clusters which presently have a short half-mass relaxation time are at the phase of complete dis-

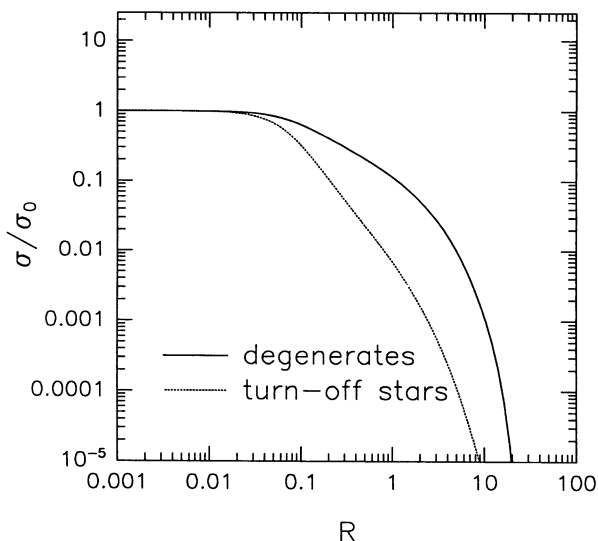


FIG. 9.—The projected density distribution for the model appearing in Fig. 8 at the epoch indicated by the arrow in that figure. At this time, degenerate stars account for $\sim 25\%$ of the total mass.

ruption. One signature of this will be a flattening of the mass function. The shape of the mass function within the half-mass radius can be reversed if the initial mass function was sufficiently shallow (i.e., $x \leq 1$).

The half-brightness radius in a postcollapse cluster containing massive degenerate stars may be resolvable, at least in those clusters with a relatively small mass.

We would like to thank Douglas Heggie for useful discussions. We also thank Gordon Drukier for sharing certain of his results pertaining to gravothermal oscillations in multi-component clusters. This research has been supported in part by the Natural Sciences and Engineering Research Council of Canada and in part by the nondirected research fund of the Korea Research Foundation in 1989.

REFERENCES

- Allen, A. J., and Richstone, D. O. 1988, *Ap. J.*, **325**, 583.
 Binney, J., and Tremaine, S. 1988, *Galactic Dynamics* (Princeton: Princeton University Press).
 Chernoff, D. F., and Shapiro, S. L. 1988, in *IAU Symposium 126, Globular Cluster Systems in Galaxies*, ed. J. Grindlay and A. G. D. Phillip (Dordrecht: Kluwer), p. 2, 3.
 Chernoff, D. F., and Weinberg, M. D. 1990, *Ap. J.*, **351**, 121.
 Cohn, H. N. 1985, in *IAU Symposium 113, Dynamics of Star Clusters*, ed. J. Goodman and P. Hut (Dordrecht: Reidel), p. 161.
 Cohn, H., Hut, P., and Wise, M. 1989, *Ap. J.*, **342**, 814.
 Djorgovski, S. G., and King, I. P. 1986, *Ap. J. (Letters)*, **305**, L61.
 Fahlman, G. G., Richer, H. B., and Drukier, G. A. 1990, in preparation.
 Fahlman, G. G., Richer, H. B., Searle, L. and Thompson, I. B. 1989, *Ap. J. (Letters)*, **343**, 49.
 Goodman, J. G. 1987, *Ap. J.*, **313**, 576.
 Goodman, J. G. 1988, in *Dynamics of Dense Stellar Systems*, ed. D. Merritt (Cambridge: Cambridge University Press), p. 183.
 Heggie, D. C., and Ramamani, N. 1989, *M.N.R.A.S.*, **237**, 757.
 Henon, M. 1961, *Ann. d'Ap.*, **24**, 369.
 Iben, I., and Renzini, A. 1983, *Ann. Rev. Astr. Ap.*, **21**, 271.
 Inagaki, S., and Lynden-Bell, D. 1983, *M.N.R.A.S.*, **205**, 913.
 Larson, D. 1984, *M.N.R.A.S.*, **210**, 763.
 Lee, H. M. 1987a, *Ap. J.*, **319**, 772.
 ———. 1987b, *Ap. J.*, **319**, 801.
 Lee, H. M., Heggie, D. C., and Ostriker, J. P. 1990, in preparation.
 Lee, H. M., and Ostriker, J. P. 1987, *Ap. J.*, **322**, 123.
 McClure, R. D., et al. 1986, *Ap. J.*, **307**, L49.
 McMillan, S. L. W. 1986, *Ap. J.*, **306**, 552.
 Meylan, G. 1988, *Astr. Ap.*, **191**, 215.
 Murphy, B. W., Cohn, H., and Hut, P. 1989, *Bull. A.A.S.*, **21**, 791.
 ———. 1990, preprint, *M.N.R.A.S.*, in press.
 Ostriker, J. P. 1985, in *IAU Symposium 113, Dynamics of Star Clusters*, ed. J. Goodman and P. Hut (Dordrecht: Reidel), p. 347.
 Pryor, C., McClure, R. D., Fletcher, J. M., and Hesser, J. E. 1989, *A.J.*, **98**, 596.
 Pryor, C., Smith, G. H., and McClure, R. D. 1986, *A.J.*, **92**, 1358.
 Richer, H. B., and Fahlman, G. G. 1989, *Ap. J.*, **339**, 178.
 Spitzer, L. Jr. 1988, *Dynamical Evolution of Globular Clusters* (Princeton: Princeton University Press).
 Spitzer, L., Jr., and Hart, M. H. 1971, *Ap. J.*, **166**, 483.
 Statler, T. S., Ostriker, J. P., and Cohn, H. N. 1987, *Ap. J.*, **316**, 626.
 Stodolkiewicz, J. S. 1985, in *IAU Symposium 113, Dynamics of Star Clusters*, ed. J. Goodman and P. Hut (Dordrecht: Reidel), p. 361.

GREGORY FAHLMAN and HARVEY RICHER: Department of Geophysics and Astronomy, University of British Columbia, Vancouver, Canada, BC V6T 1W5

HYUNG MOK LEE: Department of Earth Sciences, Pusan University, Pusan 609-735, Korea